

Number-resolving photon detectors with atoms coupled to waveguides

Daniel Malz and J. Ignacio Cirac

Max Planck Institute for Quantum Optics, Hans-Kopfermann-Straße 1, D-85748 Garching, Germany and
Munich Center for Quantum Science and Technology, Schellingstraße 4, D-80799 München, Germany

(Dated: May 5, 2022)

Number-resolving single-photon detectors represent a key technology for a host of quantum optics protocols, comprising quantum state preparation, quantum metrology, entanglement distribution, and quantum computing. Despite significant advances over the last few decades, state-of-the-art technology can distinguish only very low photon numbers with high fidelity. We show that (artificial) atoms coupled to photonic waveguides constitute an ideal platform to entirely absorb incident photonic wavepackets, even in the presence of disorder and finite Purcell factors, with a fidelity increasing with the number of atoms. Absorption is achieved through engineering a decay channel to a metastable state, such that readout of the atomic state after absorption yields a number-resolving measurement of photon number.

Introduction.—Single-photon detectors have a long history [1], with a plethora of technologies available [2]. Applications in quantum optics, such as quantum state preparation, quantum metrology [3], entanglement distribution [4], and quantum computing [5, 6] have placed a renewed focus on single-photon detectors capable of resolving the number of incoming photons. Perhaps the most promising technology in this regard are superconducting transition-edge sensors, which have been demonstrated to achieve a (per-photon) detection efficiency (percentage of detected photons) of $\eta \approx 95\%$ [7] and to distinguish up to seven photons, with a negligible dark count rate (clicks in the absence of incoming photons). They are based on the principle that near the critical temperature, the resistance of a superconductor is very sensitive to temperature changes, down to the level of single photon energies. While very impressive, this still implies that for a pulse containing seven photons, there is a 30% chance of losing one.

Another—rarely pursued—strategy, which does not rely on direct or indirect energy measurements, can generically be described as a setup in which incoming photons interact with a local degree of freedom that can be measured with a strong measurement, such as the state of a few-level system. This may enable a quantum non-demolition (QND) measurement of photon number [8]. A proposal along those lines is to use electromagnetically-induced transparency to trap a light pulse (temporarily) in an atomic cloud, such that the number of photons can be read out by measuring how many atoms are in a particular state [9]. However, reliably detecting the state of a few atoms in a large cloud is challenging, leading to measurement errors that reduce key figures of merit.

In recent years, quantum emitters coupled to one-dimensional waveguides have emerged as a powerful experimental paradigm [10, 11]. Examples of such systems include cold atoms levitated near optical fibres [12, 13] or photonic crystal waveguides [14], but also solid-state realizations such as quantum dots [15, 16], superconducting qubits [17, 18], or NV centres [19–21]. As a result of the strong confinement of light, even a single atom can have a profound effect on light propagation, and many atoms show remarkable collective effects [22]. At the same time, impressive experimental breakthroughs have enabled the control [23] and, in particu-

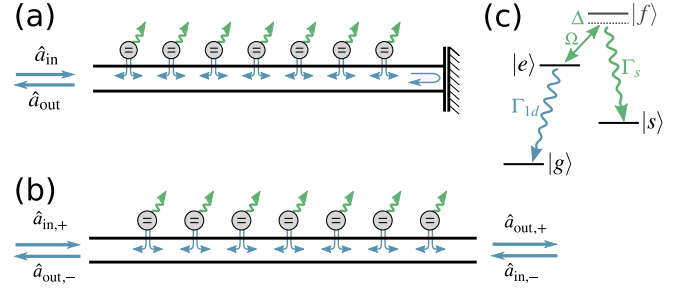


FIG. 1. Sketch of the proposed setups. We both consider atomic arrays coupled to (a) a semi-infinite waveguide terminated by a mirror at $x = 0$ and (b) an infinite waveguide. A key ingredient in the detectors is an engineered decay channel from the excited $|e\rangle$ to a metastable state $|s\rangle$, which can be implemented as a Raman transition as illustrated in (c).

lar, readout of atoms [24], superconducting circuits [25], or trapped ions [26] with essentially unity fidelity (99.94% in arrays of 160 atoms in recent experiments [24]). Thus, quantum emitters appear to be ideally suited for number-resolving detectors of photons in waveguides.

However, there is a subtlety here: While it is clear that atoms do absorb photons of certain wavelengths by going from their ground state $|g\rangle$ to an excited state $|e\rangle$, the rate at which this photon is re-emitted is typically equal to or larger than the absorption rate. In the end, the atom is again in the ground state and the information about the presence of the photon is lost. For the absorption to be *irreversible*, another decay channel needs to be present in the system. Furthermore, this decay channel needs to be such that the atom decays to a *different* state $|s\rangle$ (which needs to be metastable), such that the number of atoms in $|s\rangle$ yields information about the initial photon number.

Here, we show how such a second decay channel can be engineered such that each photon is absorbed and recorded by an atom. Even with moderate Purcell factor (ratio of waveguide to free-space decay rate), we find that detection efficiencies $\eta > 99\%$ can be reached for intermediate numbers of atoms ($N > 20$), as a consequence of collective enhancement in the atom-waveguide coupling. More surprisingly, we find

that in *any* array, even when it is entirely disordered, it is possible to engineer dissipation to achieve full absorption and arbitrarily high detection efficiencies with increasing atom number. The detection bandwidth scales with the collectively enhanced decay rate and thus also benefits from increasing atom number. The remarkable robustness against disorder establishes that even solid-state implementations of our scheme are promising candidates for high-fidelity photon counters.

Absorption in atomic arrays.—We first illustrate the general principle of photon absorption in an atomic array coupled to a one-dimensional waveguide. Below, we consider both infinite waveguides (Fig. 1b) and semi-infinite waveguides terminated by a mirror (Fig. 1a), but the principle remains the same. A key ingredient in our proposal is dissipation, which arises as engineered decay of the excited state $|e\rangle$ to a third, metastable state $|s\rangle$, as is sketched in Fig. 1(c). This is done by driving a forbidden transition from $|e\rangle$ to some auxiliary state $|f\rangle$ that decays to a fourth level $|s\rangle$, but neither to $|g\rangle$ nor to $|e\rangle$. After adiabatic elimination of $|f\rangle$, this process is described by additional decay channel from $|e\rangle$ to $|s\rangle$, with a tuneable rate. We discuss experimental details further below and in the Supplementary Information (SI).

A generic Hamiltonian describing the system-waveguide interaction is given through

$$H = \int_0^\infty \frac{dk}{2\pi} \sum_\nu (\omega_k - \omega_0) a_{\nu,k}^\dagger a_{\nu,k} - \sum_{n,\nu} g_{\nu,n} \sigma_{eg}^{(n)} a_{\nu,k} + \text{H.c.} \quad (1)$$

In Eq. (1), the label ν runs over different sets of waveguide modes, and the individual modes are labelled by their wavevector k . In an infinite waveguide (Fig. 1b), $g_{\nu,n} = \sqrt{2c\Gamma_{1d}} \exp(ik\nu x_n)$ and $\nu \in \pm$, corresponding to left- and right-moving modes, whereas for the semi-infinite waveguide (Fig. 1a), there is only one set of waveguide modes with coupling $g_k = \sqrt{c\Gamma_{1d}} \sin(kx_n)$. In these expressions, Γ_{1d} is the decay rate of an individual atom into the waveguide, and $\omega_k = ck$. Integrating out the bath modes yields quantum Langevin equations for the spin operators, which we linearize using a Holstein-Primakoff transformation, valid for small numbers of excitations in the atomic chain [10, 27–29] (for details, we refer to the SI)

$$\dot{\mathbf{b}} = (-iH_{\text{eff}} - \Gamma'/2)\mathbf{b} + \mathbf{L}\mathbf{a}_{\text{in}}. \quad (2)$$

In Eq. (2), the vector \mathbf{b} contains lowering operators for the (bosonized) N atoms, the non-Hermitian Hamiltonian H_{eff} describes both coherent interaction and decay into the waveguide, and the coupling of each mode to the input operator \mathbf{a}_{in} is given by the generically non-square matrix \mathbf{L} . In the infinite waveguide, $\mathbf{a}_{\text{in}} = (a_{\text{in},+}, a_{\text{in},-})$, such that \mathbf{L} is a $N \times 2$ matrix, whereas in the semi-infinite waveguide, there is only input mode, such that \mathbf{L} is a vector. In Eq. (2) we have already explicitly included the additional decay channels, which consists of engineered and free-space decay at rate $\Gamma' = \Gamma_{\text{eng}} + \Gamma_{\text{free}}$. More generally, Γ' could be a Hermitian matrix without invalidating the following conclusions, but we only consider uniform dissipation here for simplicity. Strictly speaking, the

engineered decay removes the atom rather than de-exciting it, but this effect is neglected in the linearization. The Langevin equations are accompanied by input-output equations

$$\begin{aligned} \mathbf{a}_{\text{out}}(\omega) &= \left\{ 1 - \mathbf{L}^\dagger [(\Gamma'/2 - i\omega)\mathbb{1} + iH_{\text{eff}}]^{-1} \mathbf{L} \right\} \mathbf{a}_{\text{in}}(\omega) \\ &\equiv \mathbf{S}(\omega)\mathbf{a}_{\text{in}}(\omega). \end{aligned} \quad (3)$$

A useful detector will count the number of photons in a specific input port (photons impinging on the system from the left, say). This is captured by our key figure of merit, the *detection efficiency* η , which is the product of the probability that a (right-moving, say) photon in the waveguide is absorbed $p_{\text{abs}} = 1 - \sum_{\nu=\pm} |\mathbf{S}_{\nu 1}(\omega)|^2$, and the probability that it is dissipated via the engineered channel rather than into free space, $\eta = p_{\text{abs}}\Gamma_{\text{eng}}/(\Gamma_{\text{end}} + \Gamma_{\text{free}})$. Thus, we require both $\Gamma_{\text{eng}} \gg \Gamma_{\text{free}}$ and $p_{\text{abs}} \approx 1$.

The latter condition is fulfilled if one of the eigenvalues of the scattering matrix $\mathbf{S}(\omega)$ is zero. This corresponds to a pole of the inverse scattering matrix $\mathbf{S}^{-1} = [1 + \mathbf{L}^\dagger(-i\omega + iH_{\text{eff}}^\dagger + \Gamma'/2)^{-1}\mathbf{L}]$ (for a proof, see SI). A pole of \mathbf{S}^{-1} arises whenever ω coincides with an eigenvalue of $H_{\text{eff}}^\dagger - i\Gamma'/2$. We can immediately conclude that the scattering matrix \mathbf{S} has a zero if $\omega - i\Gamma'/2$ coincides with an eigenvalue of H_{eff} . Perfect absorption has been observed in a variety of systems [30–32], and later been termed coherent perfect absorption (CPA) [33]. The key point here is that to reach this conclusion we did not have to assume anything about the form of H_{eff} (apart from linearity), making this a very general, robust strategy to obtain full absorption.

If these conditions are fulfilled, there exists an eigenvector \mathbf{e}_0 , such that $\mathbf{S}(\omega_0)\mathbf{e}_0 = 0$. A subtlety here is that \mathbf{e}_0 generically is a linear combination of the input modes in the various ports of the system, which is a problem in the infinite waveguide with two input modes, but not in the mirror geometry, both of which we analyze below. Nevertheless, we find that efficient detection is possible in both setups, even though full absorption in the infinite waveguide can technically only be attained in the limit of many atoms.

Mirror geometry.—In the mirror geometry, the effective Hamiltonian reads

$$H_{\text{eff},mn} = \frac{\Gamma_{1d}}{4} \left[e^{ik_0|x_m - x_n|} - e^{ik_0(x_m + x_n)} \right]. \quad (4)$$

where, as before, Γ_{1d} is single-atom decay rate into the waveguide, x_n the position of the n th atom, and k_0 is the wavevector of the emitted light (wavelength $\lambda = 2\pi/k_0$). The coupling of the atoms via the waveguide contain both a term due to photons travelling directly in between them, accumulating a phase $k_0|x_m - x_n|$, and one mediated by photons being reflected from the mirror, which incurs a minus sign and a phase $k_0(x_m + x_n)$. Since there is only one input and output field [cf. Fig. 1a], the matrix \mathbf{L} is now a vector $\mathbf{L}_n = \sqrt{\Gamma_{1d}} \sin(k_0 x_n)$.

It is instructive to see an example of how perfect absorption manifests in this setup. Placing the atoms in the atomic mirror configuration at positions $x_n = (1/4 + n)\lambda$ (due to the infinite

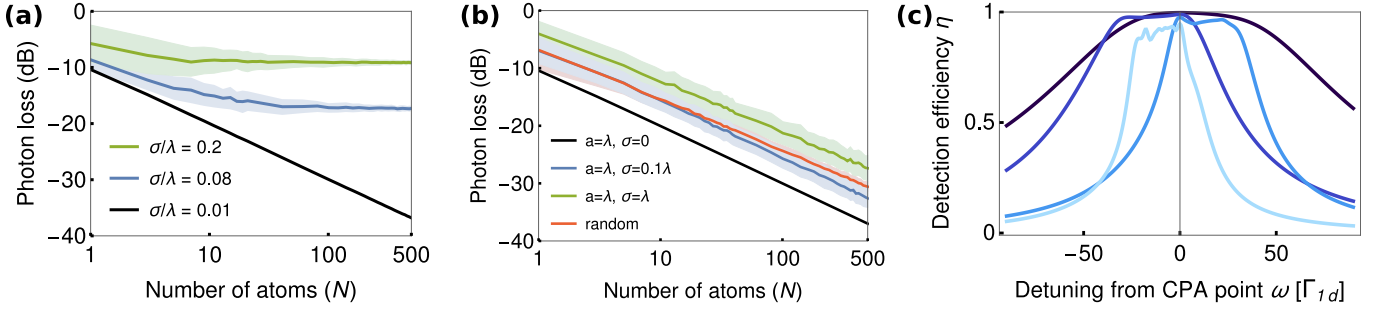


FIG. 2. Photon detection in mirror geometry. **(a)** Photon loss rate ($p_{\text{loss}} = 1 - \eta$) on resonance as a function of atom number N for a detector based on the atomic mirror configuration (lattice spacing $a = \lambda$) in the presence of weak (black), intermediate (blue) and strong (green) spatial disorder (averaged over a normal distribution with standard deviation $\sigma \equiv \sqrt{\langle \delta x^2 \rangle} = \{0.01, 0.08, 0.2\}\lambda$, where λ is the wavelength of light). The standard deviation of each curve is shown as lightly shaded area. **(b)** Same system as (a), but with engineered dissipation set to the average expected maximum dissipation rate $\Gamma_{\text{eng}} = \text{Im}[\langle \mu \rangle_{\sigma, N}]$, which mitigates the saturation in detection efficiency. We additionally show the result for a completely random array with fixed (characterizable) disorder in red. **(c)** Detection efficiency including bandwidth for completely disordered array of 200 atoms when tuned to the first, second, third, and fourth eigenvalue (from dark to light blue). This illustrates that both detection bandwidth and efficiency are optimal when choosing the most dissipative eigenvalue, as we do everywhere else in this article. Purcell factor for all plots is $P = \Gamma_{1d}/\Gamma_{\text{free}} = 10$.

range interactions, the lattice need not have unity filling), the photonic field only couples to the symmetric collective atomic excitation $B = \sum_n b_n$, which at the same time is an eigenmode of the atomic array. All other modes are dark and do not participate in the dynamics. In terms of this collective mode, the governing equations reduce to the input-output equations for a one-sided cavity [34] with internal dissipation

$$\dot{B}(t) = -\frac{\Gamma_{\text{tot}}}{2} B(t) + \sqrt{N\Gamma_{1d}} a_{\text{in}}(t), \quad (5a)$$

$$a_{\text{out}}(t) = a_{\text{in}}(t) - \sqrt{N\Gamma_{1d}} B(t), \quad (5b)$$

where we have introduced the total decay rate $\Gamma_{\text{tot}} = N\Gamma_{1d} + \Gamma'$. Solving Eq. (5a) in frequency space, the number of photons in the output field is

$$\langle a_{\text{out}}^\dagger(\omega) a_{\text{out}}(\omega) \rangle = \left| 1 - \frac{N\Gamma_{1d}}{\Gamma_{\text{tot}}/2 - i\omega} \right|^2 \langle a_{\text{in}}^\dagger(\omega) a_{\text{in}}(\omega) \rangle. \quad (6)$$

If the engineered decay is tuned such that $\Gamma_{\text{tot}} = 2N\Gamma_{1d}$, there is perfect absorption on resonance ($p_{\text{abs}} = 1$), with a bandwidth of $2N\Gamma_{1d}$. Since $\Gamma_{\text{eng}} \propto N$, as the atom number is increased, the detection efficiency $\eta = p_{\text{abs}}\Gamma_{\text{eng}}/(\Gamma_{\text{eng}} + \Gamma_{\text{free}})$ can become arbitrarily close to 1.

In Fig. 2a we include spatial disorder and show how the photon loss $p_{\text{loss}} \equiv 1 - \eta$ scales with atom number. Clearly, while it works very well for low spatial disorder ($\sigma/\lambda < 1\%$), the discussed setup suffers significantly from disorder. In the following we show how this is mitigated.

Disorder shifts the energies and decay rates of the eigenmodes of the atomic array. As a result, many collective atomic modes couple to the input field. Yet, as we have shown following Eq. (3), full absorption can be attained generically, independent of disorder. Since this relies on tuning dissipation to a specific eigenmode, which are not known *a priori*, this appears infeasible. Surprisingly, one can still vastly improve

over the results of the atomic mirror configuration, if the standard deviation $\sigma \equiv \sqrt{\langle \delta x^2 \rangle}$ of atomic positions is known. For a given N, σ , one can calculate the average largest eigenvalue $\langle \mu \rangle_{N, \sigma}$ and tune the engineered dissipation to its imaginary part $\Gamma_{\text{eng}} = \text{Im}[\langle \mu \rangle_{\sigma, N}]$. This restores the favourable scaling of detection efficiency with N , as illustrated by the orange ($\sigma = .1\lambda$) and green ($\sigma = \lambda$) curves in Fig. 2b. Most strikingly, this works even in the presence of disorder on the scale of the lattice spacing $\sigma = \lambda = a$, essentially equivalent to a fully random configuration. The reason it works lies in the fact that the absorption bandwidth grows with the imaginary part of the average eigenvalue, whereas the fluctuations (the detuning from the CPA point) only grow with its square root.

If the disorder is fixed as a result of fabrication, such as in solid-state implementations, one can further improve the scaling by first characterizing the system, such that the largest eigenvalue is known. This situation is illustrated by the red curve in Fig. 2, calculated for a completely random configuration, where we have matched Γ_{eng} to the largest eigenvalue in each disorder realization.

So far, we have just discussed absorption and detection on resonance. Equally important is the detection bandwidth, given by the engineered decay rate. Similarly, the maximum detection efficiency η depends on the ratio between engineered dissipation and total decay rate. Thus, best detection is achieved when tuning to the most dissipative eigenmode, as illustrated in Fig. 2c. This is the choice we have made for all other plots in this article.

Infinite waveguide.—Let us now turn to an atomic array coupled to an infinite waveguide, which has the simpler effective Hamiltonian $H_{\text{eff}, mn} = \Gamma_{1d} \exp(ik_0|x_m - x_n|)$, since there is only one path for a photon to travel from one atom to the next. As illustrated in Fig. 1b, there are now two input and two output modes, a right-moving one (+) and a left-moving one (-). [cf. Eq. (2)]. The atomic lowering operators couple to the input

operators via the $N \times 2$ matrix $L_{n,\nu} = \sqrt{\Gamma_{1d}} \exp(ik_0 \nu x_n)$, where $\nu \in \{\pm\}$. The scattering matrix may be written

$$S(\omega) = \begin{pmatrix} 1 & 0 \\ 0 & 1 \end{pmatrix} - \begin{pmatrix} \mathbf{L}^\dagger \mathbf{M}^{-1}(\omega) \mathbf{L} & \mathbf{L}^\dagger \mathbf{M}^{-1}(\omega) \mathbf{L}^\dagger \\ \mathbf{L} \mathbf{M}^{-1}(\omega) \mathbf{L} & \mathbf{L} \mathbf{M}^{-1}(\omega) \mathbf{L}^\dagger \end{pmatrix}, \quad (7)$$

where we have defined $\mathbf{M} \equiv iH_{\text{eff}} + i\omega + \Gamma'/2$ and the vector $\mathbf{L} \equiv \mathbf{L}_+$ for brevity (note $\mathbf{L}_+ = \mathbf{L}^\dagger$). Since \mathbf{M} is symmetric, transmission of right- and left-moving waves (the diagonal elements of S) are equal.

In this geometry, CPA does not imply $p_{\text{abs}} = 1$. For example, in the atomic mirror configuration (lattice spacing $a = \lambda$), tuning to CPA ($\Gamma_{\text{eng}} = N\Gamma_{1d}$) yields an amplitude scattering matrix on resonance

$$S_{\text{AMC}}(\omega = 0) = \frac{1}{2} \begin{pmatrix} 1 & -1 \\ -1 & 1 \end{pmatrix}. \quad (8)$$

This gives perfect absorption for symmetric wavepackets, but not for wavepackets incident from one direction. The latter requires $S \rightarrow 0$. For this reason, the atomic mirror configuration is not suited to build a detector.

Instead, any other lattice spacing will do, which is shown explicitly in the SI. Similar considerations apply as in the mirror geometry, which we have placed in the SI to avoid repetition. The upshot is that arbitrary detection efficiencies can again be attained by increasing atom number, independent of disorder.

Chiral waveguide.—Interestingly, in the recently demonstrated platforms for chiral atom-waveguide coupling [35] are another architecture in which robust photon detection may be achieved. This situation describes a range of situation, for example when the light field is strongly confined [36–38], or when giant atoms are tuned to give a chiral coupling [39].

By design, (almost) no backscattering occurs in these systems, there are no collective effects, and the spacing of the atoms is immaterial, making the analysis straightforward. Clearly, the probability for an incoming photon to pass N quantum emitters decreases exponentially with N , $|T|^2 = |t|^{2N}$. In the limit of large N and in the almost directional regime, $\gamma_+ \gg \gamma_-$, where γ_\pm are the coupling rates to right- and left-moving photons, the detection efficiency η is given to first order in γ_-/γ_+ by (derivation in SI)

$$\eta_{\text{chiral}} = \frac{\Gamma_{\text{eng}}}{\Gamma'} \left(1 - \frac{\gamma_-}{\gamma_+ + \Gamma'} \right). \quad (9)$$

Experimental considerations.—A tacit assumption in our discussion so far has been that the engineered decay Γ_{eng} can be arbitrarily tuned, even though ultimately it is limited by the decay rate to the metastable state Γ_s , such that generically $\Gamma_{\text{eng}} \sim \Gamma_{\text{free}}$, severely limiting the detection efficiency η . In solid-state systems, this may be overcome by designing a band-structure for light with a high density of states at the transition frequency from $|f\rangle$ to $|s\rangle$, whereas in atomic systems it may be possible to choose $g \leftrightarrow e$ to be a narrow transition.

A more flexible solution is shown in Fig. 3 and consists of replacing the direct transition from $|g\rangle$ to $|e\rangle$ by another Raman transition, which yields a tuneable waveguide decay rate

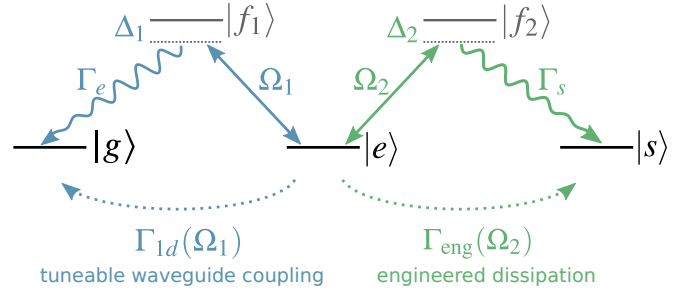


FIG. 3. Extended level scheme including two Raman transitions that allows Γ_{1d} and Γ_{eng} to be tuned independently of each other.

$\Gamma_{1d}(\Omega_1)$. If $|e\rangle$ is chosen to be a hyperfine state that does not decay to $|g\rangle$, the Purcell factor $\Gamma_{1d}/\Gamma_{\text{free}}$ is fixed, but Γ_{1d} and Γ_{free} can be tuned independently from Γ_{eng} . Ultimately, Γ_{eng} still limits detection bandwidth, but not detection efficiency. Analyzing the effect of decays from $|f_i\rangle$ back to $|e\rangle$ (see SI), we find that only $|f_2\rangle \rightarrow |e\rangle$ is relevant, which should therefore be minimized by choosing a forbidden transition.

An aspect we have not considered is inhomogeneous broadening—disorder in the transition energy of the quantum emitters—which is particularly pertinent in solid-state devices. This is permissible, as the relative effect of disorder decreases as the number of atoms increases. Even if inhomogeneous broadening is not negligible, it does not prevent full absorption, though the collective decay and thus η may be reduced.

Similar to inhomogeneous broadening, atomic motion can also lead to frequency mismatch via the Doppler shift. This is negligible, if atomic velocities (or trap frequencies) are low enough such that the resulting Doppler shift is much smaller than Γ_{eng} . If this is not the case (e.g., in the absence of trapping [40]), collective effects will be suppressed to some degree, but this can be taken into account by reducing the coupling strength in Eq. (4), and thus does not invalidate the present discussion (see SI for more details).

We have also neglected the effect of nonlinearities in our analysis, on the basis that they scale as $1/N$. Their effect can be estimated as a reduction in the collective decay rate with each absorbed photon. Using Eq. (6) to estimate the effect (the reduction in decay rate is most prominent in the atomic mirror configuration), we find that absorbing m photons reduces p_{abs} by $m^2/4N^2$. Thus, assuming we start from $p_{\text{abs}} = 1$, the probability that m photons are absorbed is $1 - (2m^3 - 3m^2 + m)/24N^2$ to third order in $1/N$.

Conclusion.—In this article, we have explored the use of arrays of quantum emitters coupled to one-dimensional waveguides to achieve number-resolving photon detection. Paying particular heed to experimental limitations such as disorder and free-space decay, we have found that both can be overcome, such that there is no fundamental limitation to the achievable detection efficiency. At its core, our proposal builds on four facts that together enable highly efficient detectors: (1), few-level systems allow for strong, projective measurements of their state due to their intrinsic nonlinearity, (2), nevertheless,

sufficiently large ensembles of atoms are linear, (3), collective decay mitigates errors due to non-idealities, and (4), in linear systems one can always engineer dissipation to obtain complete absorption. We hope that single-photon detectors based on the principles outlined here will mark a step towards high-fidelity number-resolving photon detectors.

Acknowledgments.—D.M. would like to thank Adam Smith, Clara Wanjura, and Petr Zapletal for enlightening discussions. D.M. and J.I.C. acknowledge funding from ERC Advanced Grant QENOCOPA under the EU Horizon 2020 program (Grant Agreement No. 742102).

-
- [1] G. A. Morton, *RCA Rev.* **10** (1949).
 - [2] R. H. Hadfield, *Nature Photonics* **3**, 696 (2009).
 - [3] V. Giovannetti, S. Lloyd, and L. Maccone, *Nature Photonics* **5**, 222 (2011).
 - [4] N. Gisin, G. Ribordy, W. Tittel, and H. Zbinden, *Reviews of Modern Physics* **74**, 145 (2002).
 - [5] E. Knill, R. Laflamme, and G. J. Milburn, *Nature* **409**, 46 (2001).
 - [6] P. Kok, W. J. Munro, K. Nemoto, T. C. Ralph, J. P. Dowling, and G. J. Milburn, *Reviews of Modern Physics* **79**, 135 (2007).
 - [7] A. E. Lita, A. J. Miller, and S. W. Nam, *Optics Express* **16**, 3032 (2008).
 - [8] J. M. Raimond, M. Brune, and S. Haroche, *Reviews of Modern Physics* **73**, 565 (2001).
 - [9] A. Imamoglu, *Physical Review Letters* **89**, 163602 (2002).
 - [10] D. E. Chang, J. S. Douglas, A. González-Tudela, C.-L. Hung, and H. J. Kimble, *Reviews of Modern Physics* **90**, 031002 (2018).
 - [11] P. Türschmann, H. L. Jeannic, S. F. Simonsen, H. R. Haakh, S. Götzinger, V. Sandoghdar, and N. Rotenberg, *arXiv* (2019), [arXiv:1906.08565](https://arxiv.org/abs/1906.08565).
 - [12] E. Vetsch, D. Reitz, G. Sagué, R. Schmidt, S. T. Dawkins, and A. Rauschenbeutel, *Physical Review Letters* **104**, 203603 (2010).
 - [13] J. S. Douglas, H. Habibian, C. L. Hung, A. V. Gorshkov, H. J. Kimble, and D. E. Chang, *Nature Photonics* **9**, 326 (2015).
 - [14] A. Goban, C.-L. Hung, J. D. Hood, S.-P. Yu, J. A. Muniz, O. Painter, and H. J. Kimble, *Physical Review Letters* **115**, 063601 (2015).
 - [15] A. V. Akimov, A. Mukherjee, C. L. Yu, D. E. Chang, A. S. Zibrov, P. R. Hemmer, H. Park, and M. D. Lukin, *Nature* **450**, 402 (2007).
 - [16] P. Lodahl, S. Mahmoodian, and S. Stobbe, *Reviews of Modern Physics* **87**, 347 (2015).
 - [17] A. F. van Loo, A. Fedorov, K. Lalumiere, B. C. Sanders, A. Blais, and A. Wallraff, *Science* **342**, 1494 (2013).
 - [18] N. M. Sundaresan, R. Lundgren, G. Zhu, A. V. Gorshkov, and A. A. Houck, *Physical Review X* **9**, 011021 (2019).
 - [19] A. Huck, S. Kumar, A. Shakoor, and U. L. Andersen, *Physical Review Letters* **106**, 096801 (2011).
 - [20] A. Sipahigil, R. E. Evans, D. D. Sukachev, M. J. Burek, J. Borregaard, M. K. Bhaskar, C. T. Nguyen, J. L. Pacheco, H. A. Atikian, C. Meuwly, R. M. Camacho, F. Jelezko, E. Bielejec, H. Park, M. Lončar, and M. D. Lukin, *Science* **354**, 847 (2016).
 - [21] R. E. Evans, M. K. Bhaskar, D. D. Sukachev, C. T. Nguyen, A. Sipahigil, M. J. Burek, B. Machielse, G. H. Zhang, A. S. Zibrov, E. Bielejec, H. Park, M. Lončar, and M. D. Lukin, *Science* **362**, 662 (2018).
 - [22] P. Solano, P. Barberis-Blostein, F. K. Fatemi, L. A. Orozco, and S. L. Rolston, *Nature Communications* **8**, 1857 (2017).
 - [23] N. Schlosser, G. Reymond, I. Protsenko, and P. Grangier, *Nature* **411**, 1024 (2001).
 - [24] T.-Y. Wu, A. Kumar, F. Giraldo, and D. S. Weiss, *Nature Physics* **15**, 538 (2019).
 - [25] T. Walter, P. Kurpiers, S. Gasparinetti, P. Magnard, A. Potočník, Y. Salathé, M. Pechal, M. Mondal, M. Oppliger, C. Eichler, and A. Wallraff, *Physical Review Applied* **7**, 054020 (2017).
 - [26] T. P. Harty, D. T. C. Allcock, C. J. Ballance, L. Guidoni, H. A. Janacek, N. M. Linke, D. N. Stacey, and D. M. Lucas, *Physical Review Letters* **113**, 220501 (2014).
 - [27] C. Gardiner and P. Zoller, *Quantum Noise: A Handbook of Markovian and Non-Markovian Quantum Stochastic Methods with Applications to Quantum Optics*, Springer Series in Synergetics (Springer, 2004).
 - [28] D. E. Chang, L. Jiang, A. V. Gorshkov, and H. J. Kimble, *New Journal of Physics* **14**, 1 (2012).
 - [29] T. Caneva, M. T. Manzoni, T. Shi, J. S. Douglas, J. I. Cirac, and D. E. Chang, *New Journal of Physics* **17**, 113001 (2015).
 - [30] R. Yan, R. Simes, and L. Coldren, *IEEE Photonics Technology Letters* **1**, 273 (1989).
 - [31] K. Kishino, M. Unlu, J.-I. Chyi, J. Reed, L. Arsenault, and H. Morkoc, *IEEE Journal of Quantum Electronics* **27**, 2025 (1991).
 - [32] M. Cai, O. Painter, and K. J. Vahala, *Physical Review Letters* **85**, 74 (2000).
 - [33] Y. D. Chong, L. Ge, H. Cao, and A. D. Stone, *Physical Review Letters* **105**, 053901 (2010).
 - [34] M. J. Collett and C. W. Gardiner, *Physical Review A* **30**, 1386 (1984).
 - [35] P. Lodahl, S. Mahmoodian, S. Stobbe, A. Rauschenbeutel, P. Schneeweiss, J. Volz, H. Pichler, and P. Zoller, *Nature* **541**, 473 (2017).
 - [36] I. J. Luxmoore, N. A. Wasley, A. J. Ramsay, A. C. Thijssen, R. Oulton, M. Hugues, S. Kasture, V. G. Achanta, A. M. Fox, and M. S. Skolnick, *Physical Review Letters* **110**, 1 (2013).
 - [37] I. Shomroni, S. Rosenblum, Y. Lovsky, O. Bechler, G. Guendelman, and B. Dayan, *Science* **345**, 903 (2014).
 - [38] I. Söllner, S. Mahmoodian, S. L. Hansen, L. Midolo, A. Javadi, G. Kiršanskas, T. Pregnolato, H. El-Ella, E. H. Lee, J. D. Song, S. Stobbe, and P. Lodahl, *Nature Nanotechnology* **10**, 775 (2015).
 - [39] A. F. Kockum, G. Johansson, and F. Nori, *Physical Review Letters* **120**, 140404 (2018).
 - [40] J. D. Hood, A. Goban, A. Asenjo-Garcia, M. Lu, S.-P. Yu, D. E. Chang, and H. J. Kimble, *Proceedings of the National Academy of Sciences* **113**, 10507 (2016).
 - [41] D. Porras and J. I. Cirac, *Physical Review A* **78**, 053816 (2008).

Derivation of Langevin equations

We study quantum emitters coupled to a semi-infinite waveguide terminated at $x = 0$ by a mirror. First assuming that the waveguide is also terminated on the other side after a length L , the bath eigenmodes have wavefunction $\phi_n(x) = \sin(k_n x) \sqrt{2/L}$, where $k_n = \pi n/L$ for all natural n . Taking the length of the waveguide to infinity, we recover the Hamiltonian given in the main text [Eq. (1)]. Within the Holstein-Primakoff the Hamiltonian reads

$$H = \int_0^\infty \frac{dk}{2\pi} \left\{ (\omega_k - \omega_0) a_k^\dagger a_k - g \sum_n \sin(kx_n) (a_k^\dagger b_n + \text{H.c.}) \right\} \quad (10)$$

Defining the sine transform and its inverse through

$$\tilde{f}(\nu) = 2 \int_0^\infty f(t) \sin(\nu t) dt, \quad f(t) = \frac{1}{\pi} \int_0^\infty \tilde{f}(\nu) \sin(\nu t) d\nu, \quad (11)$$

we can write the field in the waveguide as

$$\phi(x, t) = \int_0^\infty \frac{dk}{\pi} \sin(kx) (a_k(t) + a_k^\dagger(t)). \quad (12)$$

Defined this way, the commutation relation $[\phi(x, t), \phi(x', t)] = \delta(x - x')$ (for positive x only) implies canonical commutation relations $[a_k(t), a_q^\dagger(t)] = 2\pi\delta(k - q)$. In terms of complex amplitudes, we have

$$a(x, t) = \int_0^\infty \frac{dk}{\pi} \sin(kx) a_k(t), \quad a_k(t) = 2 \int_0^\infty dx \sin(kx) a(x, t). \quad (13)$$

Solving the operator equations of motion

$$\dot{a}_k = -i(\omega_k - \omega_0) a_k + ig \sum_n \sin(kx_n) b_n, \quad \dot{b}_n = ig \int \frac{dk}{2\pi} \sin(kx_n) a_k. \quad (14)$$

yields

$$a_k(t) = e^{-i(\omega_k - \omega_0)t} a_k(0) + ig \int_0^t d\tau e^{-i(\omega_k - \omega_0)(t - \tau)} \sum_m \sin(kx_m) b_m(\tau). \quad (15)$$

This solution can be plugged into the equation of motion for b_n . We need the following integral

$$\begin{aligned} & \int_0^\infty \frac{d\omega}{\pi} \sin(\omega x_n/c) \sin(\omega x/c) e^{-i(\omega - \omega_0)t} \\ &= \frac{e^{i\omega_0 t}}{-4} \left[\delta\left(\frac{x_n + x}{c} - t\right) + \delta\left(\frac{x_n + x}{c} + t\right) - \delta\left(\frac{x_n - x}{c} - t\right) - \delta\left(\frac{x_n - x}{c} + t\right) \right] \\ &= \frac{e^{i\omega_0 t}}{4} \left[\delta\left(\frac{|x_n - x|}{c} - t\right) - \delta\left(\frac{x_n + x}{c} - t\right) \right], \quad \text{if } x, x_n, t > 0. \end{aligned} \quad (16)$$

The equation of motion for b_n becomes

$$\begin{aligned} \dot{b}_n(t) &= \frac{ig e^{i\omega_0 t}}{4} [a(x_n + ct, 0) - a(ct - x_n, 0)] \\ &+ \frac{g^2}{8c} \sum_m \left[e^{ik_0(x_m + x_n)} b_m \left(t - \frac{x_m + x_n}{c} \right) - e^{ik_0|x_n - x_m|} b_m \left(t - \frac{|x_m - x_n|}{c} \right) \right]. \end{aligned} \quad (17)$$

We define the input field $a_{\text{in}}(t)$ as the portion of the waveguide field that was at a position $x = ct$ at time $t = 0$ and has since travelled all the way to the atoms. Thus, $a_{\text{in}}(t) = -\sqrt{c/2} e^{i\omega_0 t} a(ct, 0)$, where the pre-factor is fixed by the commutation relations of a_{in} , up to an arbitrary phase. This yields the Langevin equation

$$\begin{aligned} \dot{b}_n(t) &= \frac{g}{4i} \sqrt{\frac{2}{c}} [e^{ik_0 x_n} a_{\text{in}}(t - x_n/c) + e^{-ik_0 x_n} a_{\text{in}}(t + x_n/c)] \\ &+ \frac{g^2}{8c} \sum_m \left[e^{ik_0(x_m + x_n)} b_m \left(t - \frac{x_m + x_n}{c} \right) - e^{ik_0|x_n - x_m|} b_m \left(t - \frac{|x_m - x_n|}{c} \right) \right]. \end{aligned} \quad (18)$$

As defined, $a_{\text{in}}(t)$ is a slow variable, so if the dynamics of the system and the bandwidth of the input state around ω_0 are slow compared to the time it takes for light to travel a distance $2x_n/c$, we can neglect the retardation, rendering our description Markovian. The same applies to the atomic lowering operators.

$$\dot{b}_n(t) = \frac{g}{\sqrt{2c}} \sin(k_0 x_n) a_{\text{in}}(t) + \frac{g^2}{8c} \sum_m \left[e^{ik_0(x_m+x_n)} - e^{ik_0|x_n-x_m|} \right] b_m(t). \quad (19)$$

In order to calculate the output field, we take the integrated equation of motion for the light field and apply a sine transform. This is essentially the same as the right-hand side of the equation of motion for b_n , except evaluated at a different point in space. Choosing this point to be $x_R + \varepsilon$, i.e., a small distance to the right of the rightmost atom, and again neglecting retardation, we find

$$\int \frac{dk}{\pi} \sin(kx) a_k(t) = -i \sqrt{\frac{2}{c}} \sin[k_0(x_R + \varepsilon)] a_{\text{in}}(t) - \frac{ig}{4c} \sum_m e^{ik_0(x_R + \varepsilon)} 2i \sin(k_0 x_m) b_m(t). \quad (20)$$

Further choosing ε such that $\sin[k_0(x_R + \varepsilon)] = 1$, and defining $a_{\text{out}}(t) = -\sqrt{c/2} e^{i\omega_0 t} a(x_R + \varepsilon, t)$, we have

$$a_{\text{out}}(t) = a_{\text{in}}(t) - \frac{g}{\sqrt{2c}} \sum_m \sin(k_0 x_m) b_m(t). \quad (21)$$

Finally, let us define the decay rate $\Gamma_{1d} = g^2/2c$.

$$\dot{b}_n(t) = \sqrt{\Gamma_{1d}} \sin(k_0 x_n) a_{\text{in}}(t) - \frac{\Gamma_{1d}}{4} \sum_m \left[e^{ik_0|x_m-x_n|} - e^{ik_0(x_n+x_m)} \right] b_m(t), \quad (22a)$$

$$a_{\text{out}}(t) = a_{\text{in}}(t) - \sqrt{\Gamma_{1d}} \sum_m \sin(k_0 x_m) b_m(t). \quad (22b)$$

The derivation for the infinite waveguide proceeds in much the same way and can be found elsewhere [29].

dissipation engineering

As is illustrated in Fig. 1, the metastable level $|s\rangle$ forms a Λ -scheme together with the auxiliary state $|f\rangle$ and the excited atomic state $|e\rangle$. Adiabatic elimination of $|f\rangle$, valid if the detuning Δ is large compared to the Rabi frequency, yields an artificial decay channel from $|e\rangle$ to $|s\rangle$. This can be modelled through the Hamiltonian

$$H = \sum_k (\omega_k - \omega_0) c_k^\dagger c_k - \left[g_{\text{diss}} \sum_n \sigma_{es}^n c_k + \text{H.c.} \right] + H_{\text{atom-waveguide}}, \quad (23)$$

where $H_{\text{atom-waveguide}}$ is the Hamiltonian given in the main text [Eq. (1)], and $\sigma_{es}^n \equiv |e\rangle_n \langle s|$. For our purposes it does not matter if $\{c_k\}$ are waveguide modes (in a different frequency range from the bandwidth of the detector), free-space modes, or some other guided modes. While it is well-known that the decay of atoms into free space does not lead to collective effects in 1D arrays of atoms in optical lattices (i.e., spaced by at least the wavelength of light), interestingly even if the transition $e \leftrightarrow s$ is coupled to a 1D waveguide, there are no collective effects that affect the detector, as we will show in the following.

A Hamiltonian that combines both bath couplings reads

$$H = \sum_{\nu=\pm} \int \frac{dk}{2\pi} \sum_{\alpha} (\omega_k - \omega_0) a_{k,\nu,\alpha}^\dagger a_{k,\nu,\alpha} - \sum_n \left[\sqrt{\Gamma_1} e^{i(\nu k - k_{L,1})x_n} \sigma_{eg}^n a_{k,\nu,1} + \sqrt{\Gamma_2} e^{i(\nu k - k_{L,2})x_n} \sigma_{es}^n a_{k,\nu,2} + \text{H.c.} \right] \quad (24)$$

There are two waveguide fields, $\alpha = 1, 2$, distinguished either in frequency, polarization, or by being in a different waveguide. From Eq. (24), we can derive the bath equations of motion, integrate them up and Fourier transform them [29]

$$a_{\nu,1}(x, t) = e^{i\omega_0 t} a_{\nu,1}(x - ct, 0) + ig_1 \Theta[(x - \nu x_n)/c] e^{ik_1(x - \nu x_n) + ik_{L,1}x_n} \sigma_{ge}^n [t - (x - \nu x_n)/c]. \quad (25)$$

For the other field, we have to exchange $1 \leftrightarrow 2$ and $g \leftrightarrow s$. As above, we next derive the atomic equations of motion

$$\dot{\sigma}_{ge}^n = \sum_{\nu=\pm} \int \frac{dk}{2\pi} (-ig_1) e^{i(\nu k - k_{L,1})x_n} a_{k,\nu,1} (\sigma_{ee}^n - \sigma_{gg}^n) + (ig_2) e^{i(\nu k - k_{L,2})x_n} a_{k,\nu,2} \sigma_{gs}^n, \quad (26a)$$

$$\dot{\sigma}_{se}^n = \sum_{\nu=\pm} \int \frac{dk}{2\pi} (-ig_2) e^{i(\nu k - k_{L,2})x_n} a_{k,\nu,2} (\sigma_{ee}^n - \sigma_{ss}^n) + (ig_1) e^{i(\nu k - k_{L,1})x_n} a_{k,\nu,1} \sigma_{sg}^n. \quad (26b)$$

and replace the photon field [Eq. (25)]

$$\begin{aligned}\dot{\sigma}_{ge}^n &= \sqrt{\Gamma_1} \sum_{\nu=\pm} e^{i(k_1\nu-k_{L,1})x_n} (\sigma_{gg}^n - \sigma_{ee}^n) a_{\text{in},\nu,1} - \Gamma_1 \sum_m e^{ik_1|x_m-x_n|-ik_{L,1}(x_m-x_n)} (\sigma_{gg}^n - \sigma_{ee}^n) \sigma_{ge}^m \\ &+ \sqrt{\Gamma_2} \sum_{\nu=\pm} e^{i(k_2\nu-k_{L,2})x_n} \sigma_{gs}^n a_{\text{in},\nu,2} - \Gamma_2 \sum_m e^{ik_2|x_m-x_n|-ik_{L,2}(x_m-x_n)} \sigma_{gs}^n \sigma_{se}^m,\end{aligned}\quad (27a)$$

$$\begin{aligned}\dot{\sigma}_{se}^n &= \sqrt{\Gamma_2} \sum_{\nu=\pm} e^{i(k_2\nu-k_{L,2})x_n} (\sigma_{ss}^n - \sigma_{ee}^n) a_{\text{in},\nu,2} - \Gamma_2 \sum_m e^{ik_2|x_m-x_n|-ik_{L,2}(x_m-x_n)} (\sigma_{ss}^n - \sigma_{ee}^n) \sigma_{se}^m \\ &+ \sqrt{\Gamma_1} \sum_{\nu=\pm} e^{i(k_1\nu-k_{L,1})x_n} \sigma_{sg}^n a_{\text{in},\nu,1} - \Gamma_1 \sum_m e^{ik_1|x_m-x_n|-ik_{L,1}(x_m-x_n)} \sigma_{sg}^n \sigma_{ge}^m,\end{aligned}\quad (27b)$$

$$a_{\text{out},\nu,1} = a_{\text{in},\nu,1} - \sqrt{\Gamma_1} \sum_n e^{i(k_{L,1}-\nu k_1)x_n} \sigma_{ge}^n, \quad (27c)$$

$$a_{\text{out},\nu,2} = a_{\text{in},\nu,2} - \sqrt{\Gamma_2} \sum_n e^{i(k_{L,2}-\nu k_2)x_n} \sigma_{es}^n. \quad (27d)$$

Linearizing, we'll replace $\sigma_{ge} \rightarrow b$, $\sigma_{gs} \rightarrow c$, $\sigma_{gg} \rightarrow 1$, $\sigma_{ee} \rightarrow 0$ (b and c being bosonic annihilation operators), and derive the equations of motion in the same vein as above

$$\begin{aligned}\dot{b}_n &= \sqrt{\Gamma_1} \sum_{\nu=\pm} e^{ik_1\nu x_n} a_{\text{in},\nu,1} - \Gamma_1 \sum_m e^{ik_1|x_m-x_n|} b_m \\ &+ \sqrt{\Gamma_2} \sum_{\nu=\pm} e^{ik_2\nu x_n} c_n a_{\text{in},\nu,2} - \Gamma_2 \sum_m e^{ik_2|x_m-x_n|} c_n c_m^\dagger b_m,\end{aligned}\quad (28a)$$

$$\begin{aligned}\dot{c}_n &= \sqrt{\Gamma_1} \sum_{\nu=\pm} e^{ik_1\nu x_n} (-b_n^\dagger c_n) a_{\text{in},\nu,1} - \Gamma_1 \sum_m e^{ik_1|x_m-x_n|} (-b_n^\dagger c_n) b_m \\ &+ \sqrt{\Gamma_2} \sum_{\nu=\pm} e^{-ik_2\nu x_n} b_n a_{\text{in},\nu,2}^\dagger - \Gamma_2 \sum_m e^{-ik_2|x_m-x_n|} b_n b_m^\dagger c_m,\end{aligned}\quad (28b)$$

$$a_{\text{out},\nu,1} = a_{\text{in},\nu,1} - \sqrt{\Gamma_1} \sum_n e^{-i\nu k_1 x_n} b_n, \quad (28c)$$

$$a_{\text{out},\nu,2} = a_{\text{in},\nu,2} - \sqrt{\Gamma_2} \sum_n e^{-i\nu k_2 x_n} b_n^\dagger c_n. \quad (28d)$$

The bosonization and indeed everything we do here is in the approximation of low excitation numbers. Thus we normal-order the non-linear terms (which picks up a commutator), and then throw away terms like $c_m^\dagger c_n b_m$, as they are small. Thus, we find

$$\dot{b}_n = \sqrt{\Gamma_1} \sum_{\nu=\pm} e^{ik_1\nu x_n} a_{\text{in},\nu,1} - \sum_m \Gamma_1 e^{ik_2|x_m-x_n|} b_m - \Gamma_2 b_n \quad (29a)$$

$$\dot{c}_n = \sqrt{\Gamma_2} \sum_{\nu=\pm} e^{-ik_2\nu x_n} b_n a_{\text{in},\nu,2}^\dagger - \Gamma_2 c_n, \quad (29b)$$

$$a_{\text{out},\nu,1} = a_{\text{in},\nu,1} - \sqrt{\Gamma_1} \sum_n e^{-i\nu k_1 x_n} b_n, \quad (29c)$$

$$a_{\text{out},\nu,2} = a_{\text{in},\nu,2} - \sqrt{\Gamma_2} \sum_n e^{-i\nu k_2 x_n} b_n^\dagger c_n. \quad (29d)$$

In the linearized regime, the decay to the metastable state is therefore simply characterized by an additional decay rate. An important point is that the atoms in a metastable state cease to participate in the dynamics such that the collective decay rate decreases accordingly, which is discussed in the main text.

Non-idealities in double Λ -system

In order to evaluate the effect of additional decays from $|f_1\rangle$ and $|f_2\rangle$ to $|e\rangle$, we derive the effective quantum master equation of the double- Λ shown in Fig. 4. Neglecting the energy shifts due to the pumps, the dynamics are purely dissipative, given by the

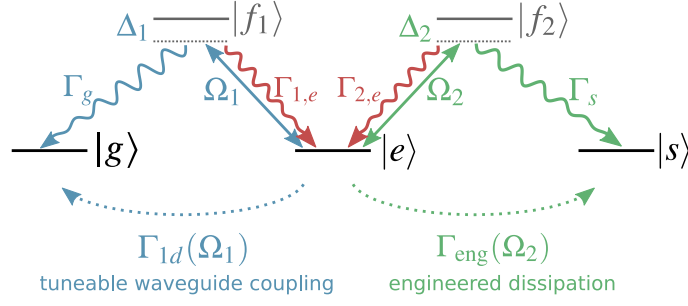


FIG. 4. The double- Λ scheme with additional decay channels from $|f_1\rangle$ and $|f_2\rangle$ back to $|e\rangle$.

jump operators

$$\hat{L}_{g,\text{eff}} = \frac{\sqrt{\Gamma_g}\Omega_1}{2\Delta_1 - i(\Gamma_g + \Gamma_{1e})}|g\rangle\langle e|, \quad \hat{L}_{s,\text{eff}} = \frac{\sqrt{\Gamma_s}\Omega_2}{2\Delta_2 - i(\Gamma_s + \Gamma_{2e})}|s\rangle\langle e|, \quad (30a)$$

$$\hat{L}_{ee,\text{eff}} = \left(\frac{\sqrt{\Gamma_{1e}}\Omega_1}{2\Delta_1 - i(\Gamma_g + \Gamma_{1e})} + \frac{\sqrt{\Gamma_{2e}}\Omega_2}{2\Delta_2 - i(\Gamma_s + \Gamma_{2e})} \right) |e\rangle\langle e|. \quad (30b)$$

We will refer to the rates corresponding to these jump operators as $\Gamma_{1d} = \Gamma_{g,\text{eff}}$, $\Gamma_{\text{eng}} = \Gamma_{s,\text{eff}}$, and $\Gamma_{ee,\text{eff}}$.

In a regime in which the decay from $|e\rangle$ to $|g\rangle$ is collectively enhanced, $\Gamma_{1d} \ll \Gamma_{\text{eng}}$ to achieve CPA conditions. Thus, the dephasing due to the decay $|f_1\rangle \rightarrow |e\rangle$ (first term in $\Gamma_{ee,\text{eff}}$) is negligible. On the other hand, the dephasing due to the decay $\Gamma_{2,e}$ has the same dependence on driving parameters (Ω_2, Δ_2) as the engineered dissipation Γ_{eng} . In order to be negligible, we require $\Gamma_{2,e} \ll \Gamma_s$, which is for example realized if $|f_2\rangle \rightarrow |e\rangle$ is a forbidden decay, as we have proposed in the main text.

Inverse scattering matrix

It can be checked explicitly that $S^{-1} = [1 + L^\dagger(-i\omega + iH_{\text{eff}}^\dagger + \Gamma'/2)^{-1}L]$ is the inverse of S . Note that now we are taking Γ' to be a matrix, for full generality. Multiplying both, we find

$$S^{-1}S = 1 - L^\dagger(-i\omega + iH_{\text{eff}}^\dagger + \Gamma'/2)^{-1}[-i(H_{\text{eff}} - H_{\text{eff}}^\dagger) + LL^\dagger](-i\omega + iH_{\text{eff}}^\dagger + \Gamma'/2)^{-1}L = 1. \quad (31)$$

The square brackets in the above expression vanish, which can be checked explicitly for the two examples in the main text. Mathematically, one can show this holds generically, since if $\Gamma' = 0$, the scattering matrix is unitary $S^{-1} = S^\dagger$ (provable, *e.g.*, from the canonical commutation relations of output and input operators), which is only true if the term in square brackets vanishes (as ω is arbitrary). Physically, this is the fluctuation-dissipation theorem, as the anti-Hermitian part of H_{eff} specifies the damping, whereas L captures how strongly the modes are coupled to the input noise operator.

Full Langevin equations

For completeness, we state here the Langevin equations without dropping the additional quantum noise terms. For the mirror geometry, they read

$$\begin{aligned} \dot{b}_n(t) = & \sqrt{\Gamma_{1d}} \sin(k_0 x_n) a_{\text{in}}(t) - \frac{\Gamma_{1d}}{4} \sum_m \left[e^{ik_0|x_m - x_n|} - e^{ik_0(x_m + x_n)} \right] b_m(t) \\ & - \frac{\Gamma_{\text{eng}} + \Gamma_{\text{free}}}{2} b_n(t) + \sqrt{\Gamma_{\text{eng}}} c_{\text{in}}(t) + \sqrt{\Gamma_{\text{free}}} d_{\text{in}}(t), \end{aligned} \quad (32a)$$

$$a_{\text{out}}(t) = a_{\text{in}}(t) - \sqrt{\Gamma_{1d}} \sum_n \sin(k_0 x_n) b_n(t), \quad (32b)$$

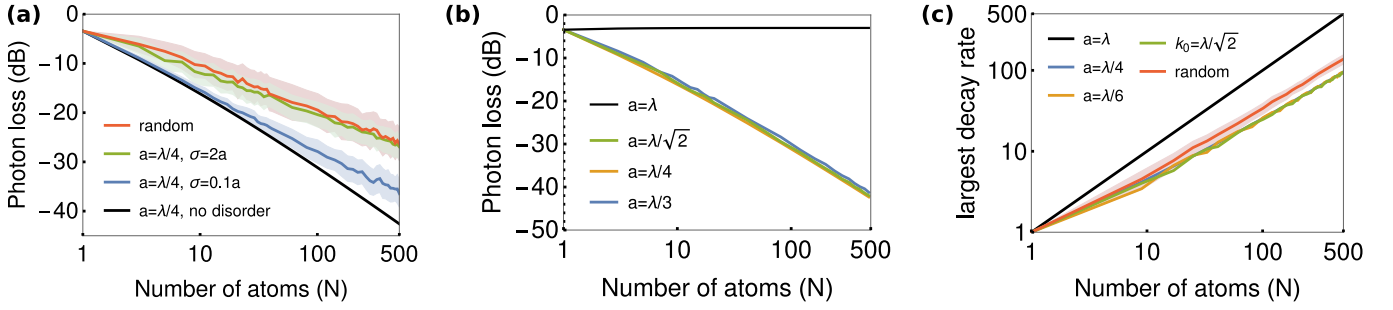


FIG. 5. **(a)** Percentage of undetected photons on resonance for an atomic array coupled to an infinite waveguide as a function of atom number. The blue line denotes the limit of a perfectly-ordered array with spacing $a = \lambda/4$ (or $5\lambda/4$ etc). Purcell factor is $P = 10$, the average for the other cases was performed over 150 disorder realization (standard deviation shown as lightly coloured area). **(b)** Detection probability for a disorder-free array of N atoms with different spacings. **(c)** Scaling of largest eigenvalue in ordered arrays with varying spacing compared to a fully random one (red). While the atomic mirror configuration ($a = \lambda$) is clearly different, it appears to be a fine-tuned exception, with all other generic arrays (ordered or disordered) behaving remarkably similar. The robustness of our scheme relies to a large degree on this universal eigenvalue scaling.

whereas for the infinite waveguide we have

$$\dot{b}_n(t) = \sqrt{\Gamma_{1d}} \sum_{\nu=\pm} e^{ik_0\nu x_n} a_{in,\nu}(t) - \Gamma_{1d} \sum_m e^{ik_0|x_m-x_n|} b_m(t) - \frac{\Gamma_{eng} + \Gamma_{free}}{2} b_n(t) + \sqrt{\Gamma_{eng}} c_{in}(t) + \sqrt{\Gamma_{free}} d_{in}(t), \quad (33a)$$

$$a_{out,\nu}(t) = a_{in,\nu}(t) - \sqrt{\Gamma_{1d}} \sum_n e^{-ik_0\nu x_n} b_n(t). \quad (33b)$$

If the modes corresponding to c_{in}, d_{in} are in vacuum, which we assume, normal-ordered expectation values involving these inputs vanish.

Infinite waveguide analysis

The scattering matrix for an array coupled to an infinite waveguide is given in Eq. (7) in the main text. One can show that for atoms arranged in a periodic array, parity symmetry implies that reflection amplitude of right- and left-moving photons differs only by a phase. This is because $\mathbf{J}\mathbf{M}\mathbf{J} = \mathbf{M}$ under the action of the exchange matrix \mathbf{J} , which consists of ones on the anti-diagonal and otherwise zeros, and $\mathbf{J}\mathbf{L} = \exp(i\phi)\mathbf{L}^\dagger$ for some ϕ . Thus, parity symmetry implies that perfect absorption may only occur if the scattering matrix is zero, corresponding to an exceptional point. In this case, we can parametrize the scattering matrix as

$$\mathbf{S}(\omega) = \begin{pmatrix} A(\omega) & B(\omega)e^{2i\phi} \\ B(\omega) & A(\omega) \end{pmatrix}, \quad (34)$$

with eigenvalues $\mu = A \pm B \exp(i\phi)$. In this system, coherent perfect absorption (one eigenvalue is zero) is equivalent to $B = \exp(i\theta)A$ and $\exp(i\phi + i\theta) = \pm 1$. In the end, full absorption of a uni-directional wavepacket may only be attained if $S = 0$. Interestingly, this happens for all arrays *except* the atomic mirror configuration [cf. Eq. (8)]. This can be deduced by estimating the magnitude of the elements of the scattering matrix through $|t|^N \sim \exp(-N^{1-\alpha})$, having assumed the decay rate of the largest eigenvalue to scale as $N^\alpha \Gamma_{1d}$. The behaviour is similar for all spacings that are sufficiently different from λ (or $\lambda/2$), including the random array. This is explicitly demonstrated in Fig. 5b,c. In the main text we take $k_0 = \pi/(2\lambda)$, as this appears to be a good choice.

Analysis of chiral waveguide

If an atom coupled to right- and left-moving modes at different rates, transmission and reflection on resonance are captured by [35]

$$\beta_\pm = \frac{\gamma_\pm}{\gamma_+ + \gamma_- + \Gamma'}, \quad t_\pm = 1 - 2\beta_\pm, \quad r_\pm = -2\sqrt{\beta_+\beta_-}. \quad (35)$$

As before, $\Gamma' = \Gamma_{\text{eng}} + \Gamma_{\text{free}}$. This allows us to calculate the absorption probability (for the +-mode)

$$A_+ \equiv 1 - |t_+|^2 - |r_+|^2 = 4\beta_+ \left(1 - \beta_+ \frac{\gamma_-}{\gamma_+} \right). \quad (36)$$

The detection probability per atom is then given through $p_{\text{detect}} = A_+ \Gamma_{\text{eng}} / \Gamma'$, while the “failure” rate is $p_{\text{loss}} = |r_+|^2 + A_+ \Gamma_{\text{free}} / \Gamma'$. In the limit of many atoms, all photons are either reflected or absorbed. To first order in γ_- , we can neglect backscattered photons. Thus, the probability that a photon is detected by the whole ensemble can be approximated to first order in γ_- / γ_+ by

$$\eta_{\text{chiral}} = \frac{p_{\text{detect}}}{p_{\text{loss}} + p_{\text{detect}}} = \left(1 - \frac{\gamma_-}{\gamma_+ + \Gamma'} \right) \frac{\Gamma_{\text{eng}}}{\Gamma'}. \quad (37)$$

Fast thermal motion of atoms

In the main text we have only considered static disorder, which is valid for slowly moving atoms. If the thermal motion of atoms is fast, some of the effect of disorder will be averaged out. This can be modelled by instead averaging the atomic coupling over a distribution of atomic positions [41]. Assuming a Gaussian distributions of positions around the atomic mirror configuration, captured by the random variable y_m

$$x_m = \frac{\pi}{k_0} \left(\frac{1}{2} + 2m \right) + y_m, \quad (38)$$

we can calculate the off-diagonal coupling

$$\bar{g}_{mn} = -\frac{\Gamma_{1d}}{8\pi\sigma^2} \iint dy_m dy_n e^{-(y_m^2 + y_n^2)/2\sigma^2} \left[e^{ik_0|y_m - y_n|} + e^{ik_0(y_m + y_n)} \right]. \quad (39)$$

If $m = n$, there should only be one integral, giving $\bar{g}_{nn} = -[1 + \exp(-k_0^2\sigma^2)]\Gamma_{1d}/(4g)$. In the case $m \neq n$, we can straightforwardly evaluate the second term, which yields $-\Gamma_{1d}e^{-k_0^2\sigma^2}/4$ overall. For the first term, we first shift $y_m \rightarrow y_m + y_n$, in which case the y_n integral becomes a straightforward Gaussian giving a factor of $\sqrt{\pi\sigma^2}e^{y_m^2/4\sigma^2}$. The leftover integral reads

$$-\frac{\Gamma_{1d}}{8\sqrt{\pi}\sigma^2} \int dy_m e^{-y_m^2/4\sigma^2} e^{ik_0|y_m|} = -\frac{\Gamma_{1d}}{4} e^{-k_0^2\sigma^2} [1 + i\text{erfi}(k_0\sigma)]. \quad (40)$$

Taken together, we get

$$\bar{g}_{mn} = -\frac{\Gamma_{1d}}{2} \left[e^{-k_0^2\sigma^2} + \frac{i}{\sqrt{\pi}} F(k_0\sigma) \right], \quad (41)$$

where $F(x)$ is the purely real Dawson integral. It is peaked at $x = 1$, is odd, and obeys $|F(x)| < 0.6$, and $F(x) \rightarrow 0^\pm$ as $x \rightarrow \pm\infty$. Equation (41) predicts that the coupling decreases exponentially in $(k_0\sigma)^2$. For low to moderate $k_0\sigma$, the effect of fast thermal motion can simply be accounted for by rescaling the couplings, without affecting the conclusions in the main text.